The EMBO Journal vol.14 no.18 pp.4551–4557, 1995

Selection of novel Mg^{2+}-dependent self-cleaving ribozymes

Kelly P.Williams[1], Stefania Ciafré and Glauco P.Tocchini-Valentini[2]

CNR Institute of Cell Biology, 43 viale Marx, 00137 Rome, Italy
[1]Present address: Whitehead Institute, Nine Cambridge Center, Cambridge MA 02142-1479, USA

[2]Corresponding author

Four RNA motifs are known that catalyse site-specific cleavage in the presence of Mg^{2+} ions, all discovered in natural RNAs. In a single *in vitro* selection experiment we have isolated representatives of five novel classes of Mg^{2+}-dependent ribozymes. Small versions of three of these showed that a very simple internal loop type of secondary structure is responsible for the activity. One of these was synthesized in a bimolecular form, and compared directly with the hammerhead ribozyme; for the new ribozyme, the cleavage step of the reaction is much faster than the spontaneous rate of phosphodiester bond cleavage, yet substantially slower than that for the hammerhead. The results suggest that many more Mg^{2+}-dependent self-cleaving RNA sequences can be found.

Keywords: hammerhead/Mg^{2+}–RNA interactions/novel ribozymes/RNA catalysis/self-cleaving RNA

Introduction

RNA is inherently less stable than DNA, because its characteristic 2′ oxygen atom can initiate a nucleophilic attack on the neighbouring phosphodiester bond; the cleavage leaves 2′,3′-cyclic phosphate and 5′-OH termini. [This is not the only pathway for RNA cleavage; for example, large ribozymes catalyse true hydrolysis (ribonuclease P RNA and side reactions of the group I and II introns), leaving 3′-OH and 5′ phosphate termini.] The 2′-O-mediated RNA cleavage reaction can be activated in various ways. Ribonuclease A employs three catalytic principles: the 2′ oxygen is deprotonated (by a basic histidine residue), the leaving 5′ oxygen is protonated (by an acidic histidine residue) and charge distribution in the transition state is stabilized by electrostatic interactions of the phosphate with a positive charge (of a lysine side chain) (Fersht, 1985). In contrast, a conformational tendency at the phosphorus toward the trigonal bipyramid geometry of the transition state may explain why 2′-O-mediated cleavage is somewhat faster within certain two-nucleotide (notably pyrimidine–adenosine) sequences (Kiersek, 1992), ostensibly in the absence of metal ions or protein catalysts; interactions between neighbouring bases may lightly constrain the conformation of the intervening phosphodiester. Divalent metal ions can also generally accelerate 2′-O-mediated cleavage, potentially acting through one or more of the principles mentioned above (metal ion-coordinated water molecules can be more readily deprotonated than in solution, and thus also participate in acid/base chemistry) (Pan *et al.*, 1993).

Strikingly, in the presence of particular divalent metal ions, certain RNA sequences undergo 2′-O-mediated cleavage at a specific site, at a rate vastly enhanced over the average rate of phosphodiester bond cleavage. Presumably the folded ribozyme provides a special binding site for the metal ion, placing it in an unusually menacing position near the fated phosphodiester bond; in some cases there is evidence that the active metal species is the hydroxide (Dahm *et al.*, 1993; Pan *et al.*, 1993, 1994). Only four distinct motifs that function with Mg^{2+} have been characterized, all discovered in natural RNAs: the hammerhead, hairpin, HDV and VS ribozymes (Pan *et al.*, 1993). Their utility as inhibitors of mRNA function is an area of active research. It has been unclear if or how many other types of self-cleaving RNA sequences might exist. Here we report the isolation of five new Mg^{2+}-dependent ribozymes from a single *in vitro* selection experiment.

The rationale of our studies was that we sought to select new types of self-cleaving RNAs in order to illuminate an unusual mode of RNA splicing, that of tRNA in eukaryotic nuclei (Phizicky and Greer, 1993). This type of splicing is notable for its dependence on characteristic exon structure: apart from the region of the anticodon loop, where the small introns are uniquely positioned, the precursors are thought to form essentially the same tertiary structure as the mature tRNA. Whereas other modes of RNA splicing appear to be primarily RNA-catalysed (by the group I and II introns themselves and, plausibly, by the RNA components of the spliceosome) and proceed by two sequential ribose-exchanging transesterifications, nuclear tRNA splicing is instead catalysed by two all-protein enzymes: an endonuclease first excises the intron with two 2′-O-mediated cleavages, after which a ligase joins the exons. This mechanism, involving termini also commonly formed by spontaneous RNA cleavage, together with the hypothesis that tRNA-like structures were important in the early evolution of nucleic acid replication systems (Weiner and Maizels, 1994), suggests that nuclear tRNA splicing may be a remnant of a process that is very ancient indeed. The 'RNA world' hypothesis, supported not least by the persistence of RNA catalysts in the other modern forms of RNA splicing, further suggests that tRNA splicing originally had RNA catalysts that were eventually supplanted by protein enzymes.

We sought to produce, by *in vitro* selection, RNA that could self-catalyse excision of its intron, hopefully dependent on tRNA-like structure in the precursor rather than specific sequences near the splice site, as an RNA-only model for the first phase of tRNA splicing. A long

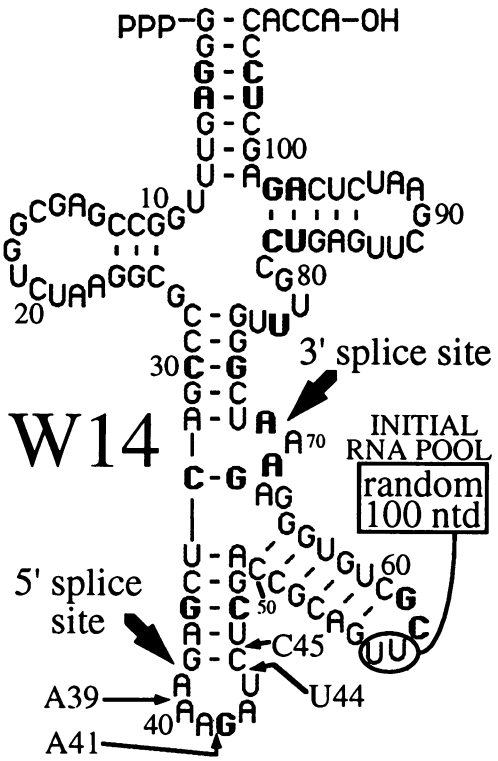

Fig. 1. Parental RNA. W14 is a multiple base substitution (changed bases shown in bold face) mutant of the ΔEA form (Baldi *et al.*, 1992) of the yeast $tRNA^{Leu3}$ splicing precursor. Sites cleaved by tRNA splicing endonuclease (thick arrows) and in the selected self-cleaving RNAs (thin arrows) are shown. The initial RNA pool for selection contained the indicated random-sequence replacement in W14.

string of random sequence was inserted in the intron of a tRNA splicing precursor, and it was hoped that some individuals in this pool could form appropriate catalytic domain(s) for cleaving both splice sites in the substrate domain of the molecule. The substrate domain was based on the yeast pre-$tRNA^{Leu3}$, which bears an intron that is somewhat longer than usual, with a 7 nt base-paired stem (positions 50–55 and 60–65 in Figure 1) that could stabilize and connect substrate and catalytic domains. Several mutations were first introduced in this precursor, however, to improve transcription by T7 RNA polymerase, create restriction sites, improve tRNA cardinal position function (Baldi *et al.*, 1992) and most importantly, to eliminate prominent sites of spontaneous breakage near the splice sites (see below).

Selection (Figure 2) was based on purification from the gel electrophoretic zone expected to contain the intron, following a long incubation of pool RNA to allow self-excision. The product was subjected to reverse transcription and amplification by PCR, facilitated by the fixed sequences at either end of the intron. A second PCR restored exons and the T7 promoter, creating transcription templates with which to initiate a subsequent selection cycle. Full-length precursor RNA was not gel-purified after transcription, in order to avoid losses of individuals that might have undergone self-excision during the transcription reaction. Note that the sequence of the entire splicing precursor domain was held fixed throughout the experiment, being regenerated in each round.

The RNAs that were eventually selected exhibited

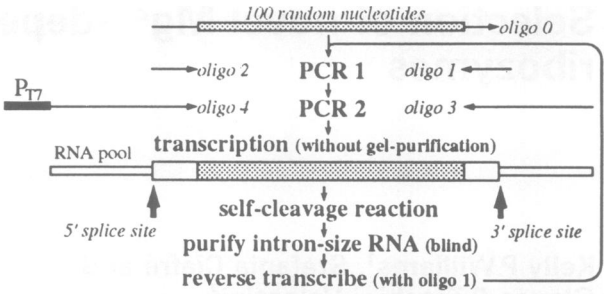

Fig. 2. Cyclical selection scheme for self-excising RNA. Sequences regenerated in each cycle are boxed in white.

reasonably strong Mg^{2+}-dependent self-cleavage near the 5′ splice site; instead, cleavage near the 3′ splice site was too slow to be clearly detected in standard self-cleavage assays. Apparently background-level cleavage near the 3′ splice site did occur during the self-cleavage step of selection, in addition to the clearly ribozymatic cleavages occurring near the 5′ splice site, thus accounting for the intron-sized RNA that was gel-purified during selection. We further characterize the new ribozymes responsible for the cleavages near the 5′ splice site.

Results

The pre-$tRNA^{Leu3}$ is susceptible to cleavage at multiple pyrimidine–adenosine sequences near the splice sites, in the absence of metal ions; these cleavages are enhanced by inclusion of polyvinylpyrrolidone in the assay buffer in the experiment of Figure 3 (Kiersek, 1992). This source of cleavage background threatened the power of our selective method, and we sought to reduce it by mutation. Several labile sites were eliminated in the multiple mutant W14 (Figure 3); one new very unstable site (C96-A97) was created, but being rather far from a splice site, it was considered less problematic for the selection experiment. The mutant retained tRNA-like features of the splicing precursor; it was cleaved by the *Xenopus* tRNA splicing endonuclease at a rate reduced <3-fold with respect to the wild-type precursor (data not shown).

Random sequence 100 nt in length was inserted in the intron of the W14 splicing precursor, and the pool RNA (originally containing ~10^{13} different sequences) was subjected to multiple rounds of selection for self-excising introns (Figure 2). A Mg^{2+}-dependent cleavage activity developed in the pool, but the product was not the size of the intron; instead, two bands of RNA closer in size to that expected from cleavage at only one splice site were produced (Figure 4). The self-cleavage activity of the pool RNA after seven rounds of selection did not appear to differ from that after six rounds. Pool DNA was cloned and 29 clones were sequenced, comprising 26 distinct sequences (Figure 5).

RNAs transcribed from these clones were assayed individually for self-cleavage activity. One sequence exhibited no activity, but each of the others tested exhibited a single prominent Mg^{2+}-dependent self-cleavage site among a few sites near but not at the authentic 5′ splice site (position G38). Most individuals cleaved at either A39 or C45; these two cleavage sites account for the two main product bands seen for the pool (Figure 4).

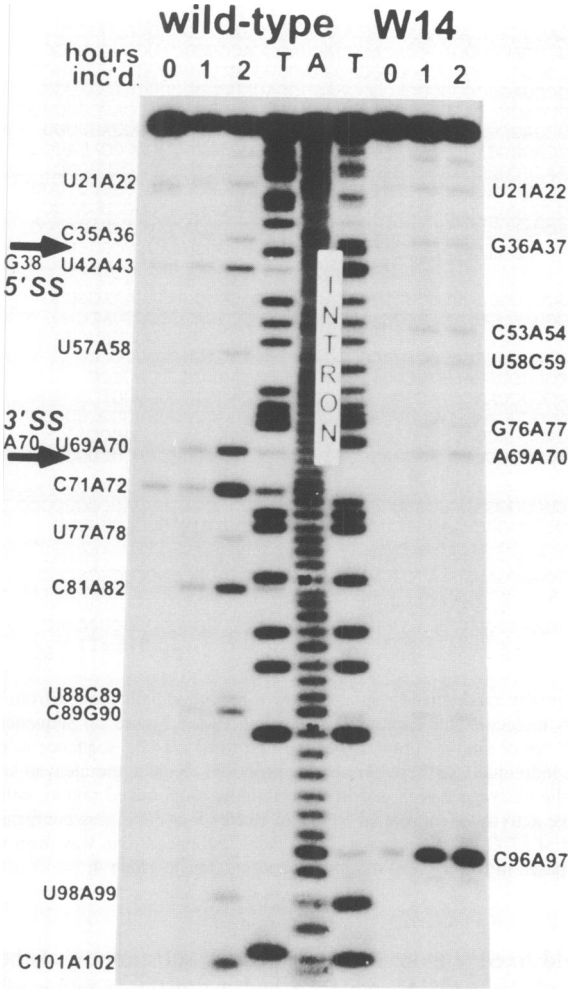

Fig. 3. Engineering RNA stability. The 3′-end-labelled ΔEA form of pre-tRNA^{Leu3} (wild-type) and the derived W14 mutant (Figure 1) were incubated in Buffer P at 37°C for the indicated reaction times; the presence of polyvinylpyrrolidone in this buffer accelerates the intrinsic cleavage rates of pyrimidine–adenosine sequences (Kiersek, 1992). Bases flanking the observed cleavage sites are given. A and T, partial alkaline and ribonuclease T1 digestions, respectively.

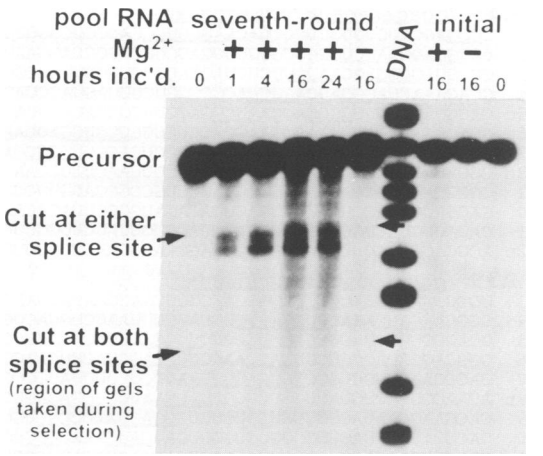

Fig. 4. Selection of Mg^{2+}-dependent self-cleavage activity. RNA from the initial pool and the pool after seven selective cycles, labelled uniformly with [^{32}P]UMP, were incubated at 30°C in Buffer S or Buffer S lacking MgOAc for the indicated times. Expected migration positions of RNA cleaved at one or both splice sites are indicated, marked using the filled-in *Hpa*II products of pBR322.

None of the selected ribozymes showed obvious sequence similarity with any of the Mg^{2+}-dependent ribozymes known from natural RNAs; instead, novel sequence motifs were associated with particular cleavage site specificities. The sequence 5′-YGG**AGCA**AUC (Y=C or U) was found in the originally randomized sequence of ten clones, associated with the C45-cleavage activity. In these RNAs, the sequence gau**c/ucga**ccg containing the cleavage site (marked by the slash) is proposed to form with the consensus a simple internal loop structure, pairing via the underlined sequences (usually forming even longer stems) and leaving the nucleotides in boldface 'looped-out':

5′gau$^{c/ucga}$ccg
3′CUA $_{ACGA}$ GGY

(We use the convention of printing sequences that were held fixed through selection in lower case, and sequences from the originally randomized region in upper case.) Clone 10 is the only C45-cutter with a variation in the **AGCA** sequence; its change of the 3′ A to C is accompanied by the only instance where the next base is G instead of A, forming the wobble instead of the Watson–Crick base-pair. In the weakly active RNA from clone 1, a much longer looped-out sequence is proposed for the non-cleaved strand; structure within the 3′ end of this region may act to present its **AGCA** sequence at the 5′ end in a conformation approaching that occurring in the more active RNAs.

Likewise, the consensus GRUY**ARDC**CUC (R=A or G; D=A,G or U) was observed in eight clones and associated with A39-cleavage activity. Again, an internal loop structure involving the cleavage site region gaga/**aa**gauc is proposed. Although the reduced consensus sequence in the A39-cleaving clone 21 would appear to pair weakly with the substrate strand, removing the element (in RNA transcribed from the *Alu*I-digested template) eliminated ribozyme activity. RNAs from two other clones cleave at A39, but appear to present a different consensus RGAU**GAAUGAWY**CGA (W=A or U) to form a larger internal loop with the cleavage region ucg**aga/aa**gaucu. Two other self-cleavage specificities, one for A41 and one for U44, were represented by single clones.

To determine whether the deduced structures indeed suffice for self-cleavage activity at A39 and C45, a small version of each motif was produced, connecting the two pairing strands by an UUCG or GAAA tetraloop (Figure 6A); the miniature ribozymes were functional (Figure 6B). Somewhat shortened forms of the RNAs cleaving at A41 (88 nt) and U44 (145 nt) were active, but attempts to further substantially shorten these ribozymes have so far yielded inactive RNAs. The experiments of Figure 6 were performed in a more simple buffer than that used during selection, demonstrating among other things that spermidine is not essential for activity of these ribozymes; the small C45 ribozyme was >10-fold more active than in the conditions used during selection. The first small version of A39b tested did not cleave to completion; the kinetics indicated that ~45% of the molecules were inactive, but that the active fraction cleaved more quickly than any of the other ribozymes (half-life, 0.8 h). Reinspection of

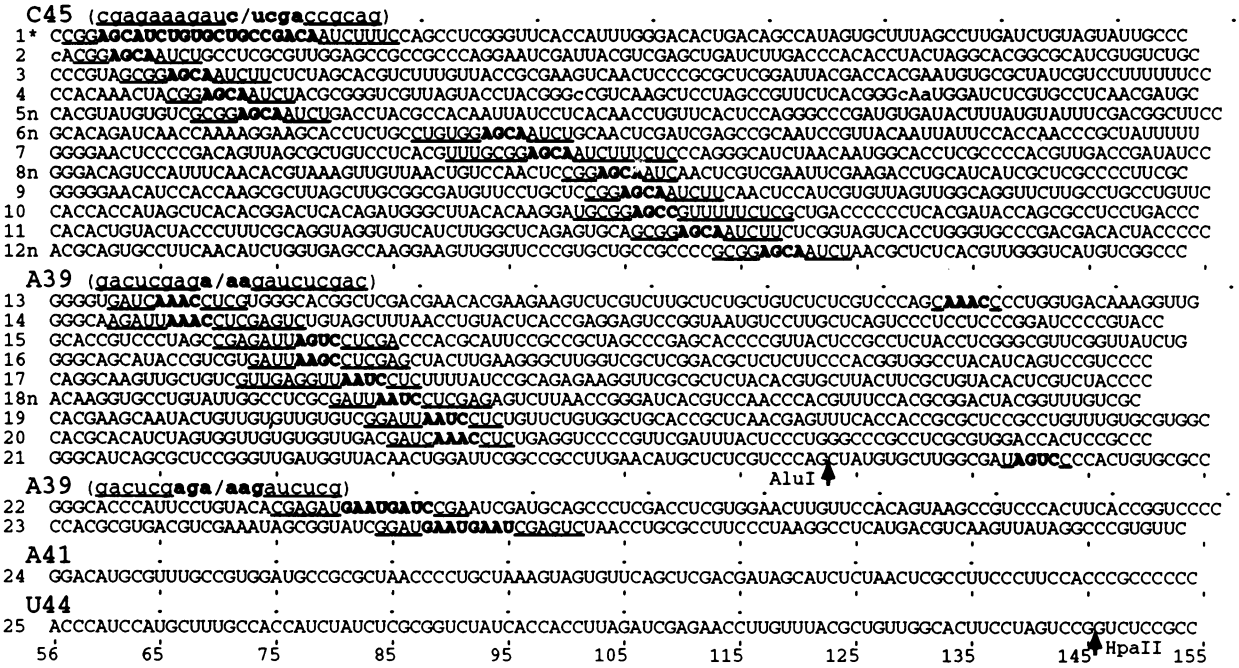

Fig. 5. Five classes of selected self-cleaving RNAs. Only the sequence of the originally randomized region is shown for individuals cloned from the pool after seven selection cycles, indexed below by its position in the whole RNA molecule (for flanking fixed sequences see Figure 1). Sequence classes are named according to the site of self-cleavage, all in the region of the 5′ splice site in Figure 1. For the first three classes, sequence in the cleavage region is shown in lower case with the cleavage site marked by a slash; individuals in these classes are proposed to place the cleaved site in an internal loop, formed by base-pairing between the underlined sequences in the cleavage region and in the originally randomized region, with nucleotides in bold looped-out (see also Figure 6A). Mg^{2+}-dependent self-cleavage activity of individual RNAs in Buffer S at 30°C was confirmed, except where not tested (n) or where weak activity was detected only in Buffer B at 37°C (*). Four other clones were sequenced: one was inactive for self-cleavage, one was identical to clone 2, one was almost identical (altered bases in lower case) to clone 2 and another to clone 4.

the sequence of A39b revealed a potential alternative secondary structure that we sought to eliminate in a second version (A39b′). However, A39b′ had only a slightly smaller apparent inactive fraction than A39b; otherwise the two versions behaved quite similarly.

The primary 5′ products of self-cleavage co-migrate with the corresponding bands of partial alkaline digests, suggesting that 2′,3′-cyclic phosphate termini are produced. This was confirmed for the miniature C45-cutter by allowing the uniformly [^{32}P]UMP-labelled RNA to self-cleave; the ratio of radioactivity in the two products showed that the phosphate of the cleavage site was transferred to the upstream product, and two-dimensional thin-layer chromatography showed that Physarum M1 ribonuclease digestion of the purified upstream cleavage product released cytidine 2′,3′-cyclic monophosphate (data not shown). A slightly faster-migrating product of the cleavage reaction was also observed (thin arrow, Figure 6B). Analysis as above identified this as the acyclic 3′(2′)-phosphate form of the upstream product; this can be generated from the 2′,3′-cyclic phosphate primary cleavage product in the absence of the rest of the ribozyme, with a half-life of 13 h (data not shown).

The multiple independent isolation of the identical looped-out **AGCA** sequence paired across from the cleavage site region in the C45-cutting clones made it clear that each of the consensus bases is important for activity. It was less clear which bases in the cleaved strand are important, since its sequence was not allowed to vary during selection. We made a brief mutational study of the miniature C45-cutter to assess these bases that had been held fixed (Figure 7). As expected, substitution of the 3′ A of the **AGCA** sequence had a drastic negative effect on activity, as did substitution at two positions in the looped-out portion of the cleaved strand. However, substitution at three of the positions in the cleaved strand, including the base immediately 5′ to the cleavage site, had less drastic effects. Substitution of either base in the presumed Watson–Crick pair near the cleavage site had deleterious effects (to different extents), but the pair-restoring double mutant had nearly parental activity.

Three of the selected ribozymes have decidedly simpler secondary structures—mere internal loops—than any of the known natural Mg^{2+}-dependent ribozymes. Nonetheless, we noticed some similarity between the hammerhead and the C45-cutter, at four bases near the cleavage site (Figure 8A). To facilitate direct comparison, we designed a double bimolecular system in which a 'substrate' RNA (S) could be cleaved at the same site by either of two 'ribozyme' RNAs (R), one pair forming the simple C45-cleavage motif and the other a hammerhead. For both combinations, single-turnover cleavage rates were measured at various concentrations of R in excess of S (Fedor and Uhlenbeck, 1992). This analysis allows the measurement of kinetic parameters according to the simple scheme:

$$S + R \leftrightarrow S{:}R \rightarrow (\text{cleaved S}){:}R$$
$$K_{M'} \qquad k_2$$

Using the C45-cleaving bimolecular ribozyme in buffer B at 37°C, $K_{M'}$ was 2×10^{-8} M and the cleavage rate

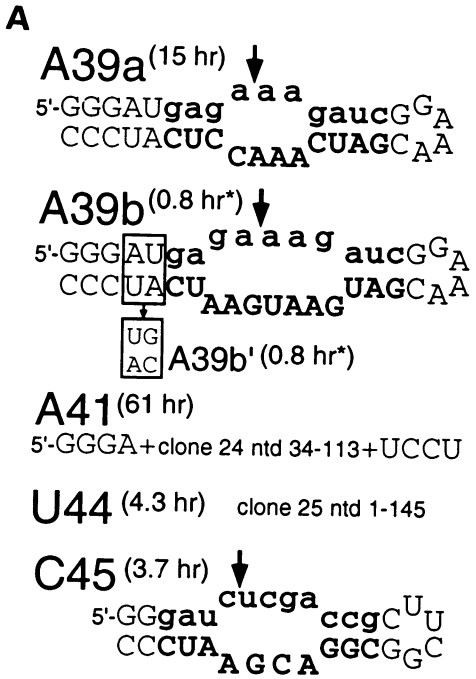

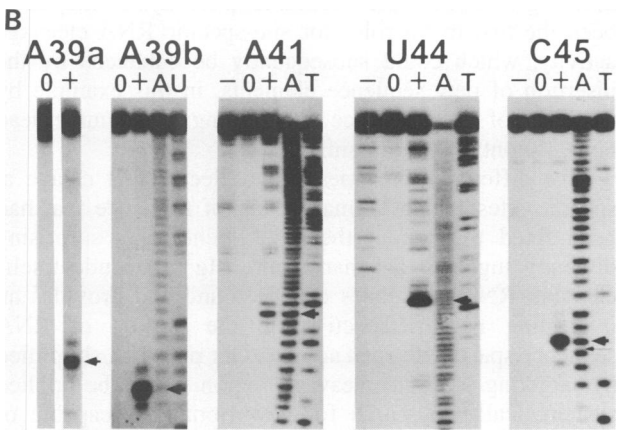

Fig. 6. Self-cleavage activity of small ribozymes. (**A**) Ribozyme sequences. Observed cleavage half-times in Buffer B at 37°C are given in parentheses; for the values marked by an asterisk the kinetic data were corrected for inactive fractions: A39b, 45% inactive; A39b', 30% inactive. (**B**) 5'-^{32}P-labelled RNAs were treated as follows: 0, unincubated RNA; +, 2 h at 37°C in Buffer B (6 h for A39a RNA); –, 2 h at 37°C in Buffer B lacking Mg^{2+}; A, T, U, partial alkaline, ribonuclease T1 or ribonuclease U2 digestions, respectively. Large arrows indicate the major cleavage product, the thin arrow marks the acyclic derivative of the 2',3'-cyclic phosphate major C45 product. This preparation of A41 exhibited ~25% contamination with an RNA shortened by one nucleotide at the 5' end.

constant k_2 was 0.2/h. Cleavage of the substrate RNA in the same conditions but with the ribozyme RNA omitted was uniform over its 16 phosphodiester bonds, and the average phosphodiester bond cleavage rate was 0.001/h; thus the C45 motif accelerated cleavage of the specific site 200-fold. For the hammerhead bimolecular ribozyme, k_2 was 100-fold greater than that for the C45 motif, whereas $K_{M'}$ was quite similar for the two ribozymes. Nonetheless, in a reaction mimicking that used during selection (Figure 8B), the hammerhead had only a 2.5-fold advantage; that is, the hammerhead cleaved nearly to

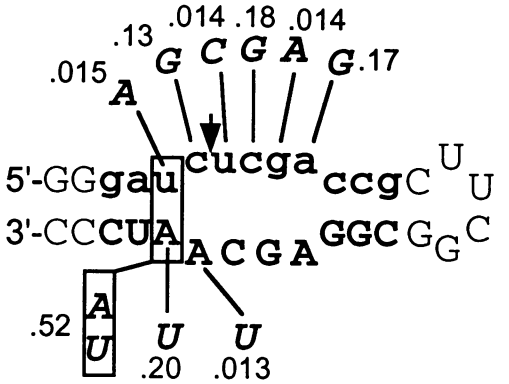

Fig. 7. Mutational analysis of the self-cleaving C45 motif. The ratio of the first-order self-cleavage rate constant k_{obs} measured in Buffer B at 37°C for several single-base and one double-base mutants with respect to that of the parental ribozyme is given.

completion, while the simple ribozyme cleaved 40% of the substrate.

Discussion

Our protocol was designed to select RNAs that self-cleave at two sites; selection was based on gel-purification of the desired intron-sized RNA, and subsequent amplification demanded that this RNA not be cut between the sequences that allow the PCR primers to bind. The search for an intron-excising RNA that depends on tRNA-like exon structure is ongoing; in this paper we report the selection of several RNAs capable of a single prominent Mg^{2+}-dependent cleavage near the tRNA 5' splice site. This fortuitous selection is most likely explained by a combination of ribozymatic cleavage near the 5' splice site and spontaneous cleavage near the 3' splice site occurring in each cycle to form good candidate molecules for passing the selective barriers. By this reasoning, the selection of five distinct ribozymes cleaving near the 5' splice site, but none cleaving near the 3' splice site, when *a priori* the selection of the two types was equally likely, might be explained by a higher rate of spontaneous breakage in the 3' splice site region than the 5' region. For example, the most abundant type of RNA near intron-size following the first self-cleavage reaction may have been the product of ribozymatic cleavage at C45 together with the strongest Mg^{2+}-independent cleavage of the substrate domain, at C96 (Figure 3); the leading edge of the gel electrophoretic band of this 149 nt RNA may have been present in the gel slice taken. In any case, regarding the selection of the singly cutting ribozymes, our gel-purification step surely constituted a major bottleneck, limiting the number of such ribozymes that could have been selected from the original pool. Our selection could not absolutely specify cleavage sites, but tended to specify cleavage regions that would leave sufficient sequence for binding PCR primers. In fact all of the selected ribozymes shortened the upstream primer-binding sequence (this may have been facilitated by the concentration of G and C residues at the proximal portion of this sequence).

That more active ribozymes were not selected in our experiment may be partly explained by more complex sequence requirements for highly active ribozymes. We

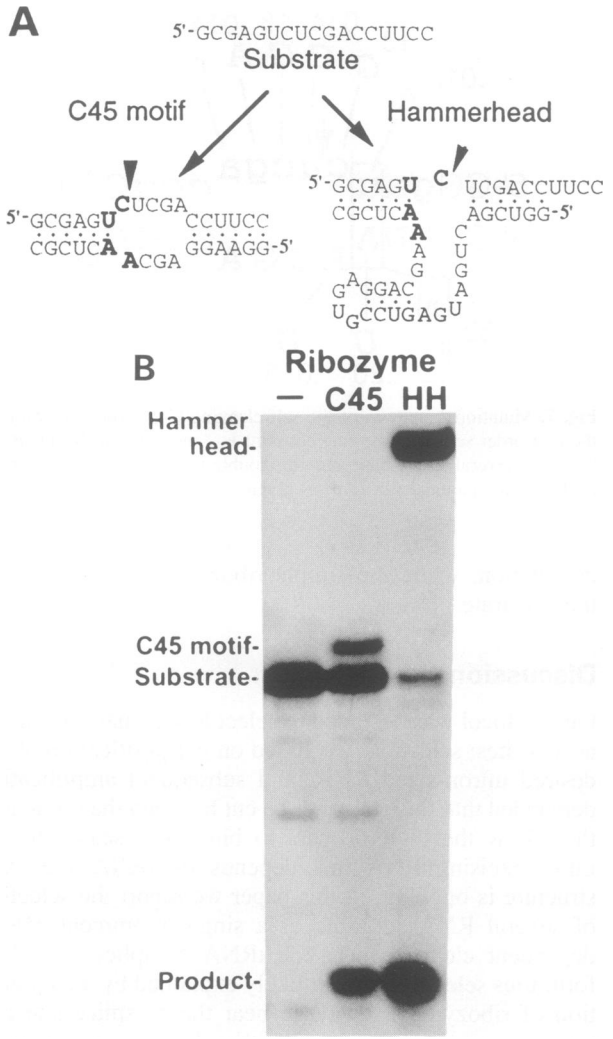

Fig. 8. Comparison of the C45 motif and the hammerhead by cleavage of the same substrate *in trans*. **(A)** Substrate and two ribozyme sequences. Similar bases between the C45 motif and hammerhead are outlined. **(B)** Comparison under selection conditions. 5′-^{32}P-labelled substrate RNA (1.25 nM) was incubated 16 h at 30°C in Buffer S alone or in the presence of 2 μM C45 or hammerhead ribozyme RNA ([^{32}P]UMP-labelled at low specific activity). Of the substrate, 40% was cleaved by the C45 motif and 94% by the hammerhead.

calculate that hammerheads cleaving at C45 would have been present in the original pool at a frequency of ~$10^{-10.5}$, 10^4 times less frequent than our simple C45-cutter. This, together with the severe bottleneck described above which lowers sequence diversity, makes it possible that no hammerheads survived the first cycle of selection. Moreover, the long reaction time employed for RNA cleavage in each cycle would have weakened the selective advantage of intrinsically more active ribozymes (Figure 8B). Similar reasoning may explain why double ribozymes cleaving near both the 3′ and 5′ splice sites were not found.

Site-specific cleavage catalysed by the new ribozymes is well above spontaneous RNA cleavage rates, yet substantially lower than that catalysed by the ribozymes known from natural RNAs. The relatively low activity of the new ribozymes does not preclude biological roles for them, such as initiating or accelerating specific mRNA decay. Weaker ribozymes may also have served as evolutionary intermediates for the more active modern ribozymes. We noted a small region of similarity between the C45-cutter and the hammerhead: both have a C as the base immediately 5′ to the cleaved phosphodiester bond, opposite from an A in the secondary structure, and the next base to the 5′ is a U opposite an A (Figure 8A). For both ribozymes, mutation of the C has only a moderate effect, but mutation of the opposite A has a drastic effect; instead, inversion of the neighbouring U:A pair to A:U has a drastic effect in the hammerhead, compared with the small effect in our ribozyme (Figure 7 and Ruffner *et al.*, 1990). The reaction mechanisms may be similar: the same cleavage products are formed and the C45 motif shows a strong pH dependence (unpublished data) which may indicate as for the hammerhead (Dahm *et al.*, 1993) that an RNA-bound Mg^{2+} hydroxide is catalytic. The lower activity may be due to suboptimal positioning of the Mg^{2+} ion with respect to the reaction centre, or alternatively, reflect a need for a slow conformational change before cleavage by the new ribozymes. Admittedly this particular similarity between a simpler ribozyme and a more active one may well be spurious, yet it serves to emphasize that strong ribozymes need not have evolved in a single step. Simple internal loop ribozymes may have been the first to fill roles for site-specific RNA cleavage activity, which could subsequently be enhanced by the insertion of new sequence elements, in this example by insertion of the sequence constituting the hammerhead helix II-containing domain.

Five different ribozymes were selected that cleave at specific sites within a small string of sequence that had been fixed throughout the experiment. This surprising diversity suggests that many more Mg^{2+}-dependent self-cleaving RNA sequences can be found and provides an interesting new perspective on the portion of RNA sequence space with such activity. Our protocol, simplified by targeting a single cleavage region, could be applied systematically to search for new ribozymes capable of cleaving desired fixed RNA sequences, for example from particular mRNAs. Furthermore, the self-cleavage step could be made much more stringent to enhance the selection of more active ribozymes.

The new ribozymes provide new materials for the study of RNA–metal ion interaction and RNA catalysis. Our experience may also serve as a warning for others using self-cleavage as a basis for selection from randomized RNA pools; even small blocks of randomized sequence may produce new ribozymes causing 2′-O-mediated cleavage near the target site.

Materials and methods

RNAs

DNA templates were either PCR products or restriction enzyme-digested plasmids containing the 17 nt T7 promoter. RNAs were transcribed using T7 RNA polymerase and purified from urea–polyacrylamide gels. RNAs were labelled either uniformly with [^{32}P]UMP, or at the 3′ end by reaction with [^{32}P]pCp and T4 RNA ligase, or at the 5′ end by treatment with phosphatase and then kinase in the presence of [γ-^{32}P]ATP. The W14 gene was created by oligonucletide-directed mutagenesis of the gene for the ΔEA form (Baldi *et al.*, 1992) of the yeast $tRNA^{Leu3}$ splicing precursor.

Initial RNA pool

It was found that ~30% of oligonucleotide 0 [W14 nt 39–55 + 100 random nt (~25% each base) + W14 nt 58–70] molecules could be

extended by DNA polymerase; 100 pmol was used as template for PCR with oligonucleotides 1 (W14 nt 39–55) and 2 (complement of W14 nt 76–58) as primers, and the product was used as template for PCR with oligonucleotides 3 (17 nt T7 promoter + W14 nt 1–55) and 4 (complement of W14 nt 109–58), with a final yield of 512 pmol. Of this DNA, 59 pmol was transcribed with a yield of 6389 pmol RNA, 1500 pmol of which was used in the first selection cycle.

Selection cycle

Pool RNA (0.1 μM, [^{32}P]UMP labelled at low specific activity) was incubated 16 h at 30°C in Buffer S (200 mM KOAc, 30 mM TrisOAc, pH 8.1, 20 mM MgOAc, 1 mM spermidine, 0.1 mM EDTA), precipitated with ethanol in the presence of 0.4 μg/ml glycogen, and subjected to electrophoresis in a thick 7 M urea/10% polyacrylamide/TBE gel alongside radioactive DNA markers (filled-in pBR322 *Hpa*II fragments). The slice of the gel expected to contain RNA of 127–133 nt was taken (the desired self-cleavage product would have been 130 nt), although a true band was never observed there. The eluted RNA was subjected to reverse transcription for 10 min at 52°C using the RNase H–MMLV enzyme (Life Technologies, Inc.) with oligonucleotide 2. RNA was degraded with alkali, and the sample was neutralized and precipitated in ethanol with glycogen. The cDNA was used as a template for PCR with oligonucleotides 1 and 2; the product was gel-purified and used as template for a second PCR with oligonucleotides 3 and 4, and the resulting templates were transcribed. Pool RNA was not gel-purified before the self-cleavage reaction.

Cleavage assay

Radioactively labelled RNAs were heated at 95°C for 1 min and cooled to 37°C at 0.1°C/min in 0.1 mM EDTA, then incubated at 1–10 nM in either Buffer S (above) at 30°C, Buffer B (50 mM Tris–Cl, pH 8.36, at 37°C, 10 mM $MgCl_2$, 0.1 mM EDTA, 0.025% Nonidet P-40) at 37°C, or Buffer P (50 mM Tris–Cl, pH 7.5, 1 mM EDTA, 1 mM spermidine, 0.1% polyvinylpyrrolidone) (Kiersek, 1992) at 37°C. Samples were subjected to electrophoresis in 7 M urea/polyacrylamide/TBE gels; fractional cleavage of ribozymes was measured using a Molecular Dynamics PhosphorImager.

Kinetic analysis of the small unimolecular ribozymes was performed in Buffer B at 37°C. For kinetic analysis of the bimolecular ribozymes, RNAs were mixed in Buffer B at 37°C (final concentration of 5′-end labelled substrate RNA, 2.5 nM; for ribozyme RNA, eight final concentrations ranging from 0.05–2 μM). Samples were taken at 1 min intervals for 5 min (hammerhead) or at 1 h intervals for 8 h (C45 motif). The cleavage rate constants were calculated and k_2 and K_M, calculated from an Eadie–Hofstee plot (Fedor and Uhlenbeck, 1992).

Acknowledgements

K.P.W. was supported by an American Cancer Society fellowship. The work was supported by Progetto Finalizzato Ingegneria Genetica (CNR), Human Frontiers Science Program Organization, and by Progetto Strategico (CNR) 'Nucleotidi antisenso come strumento di nuove strategie terapeutiche'.

References

Baldi,M.I., Mattoccia,E., Bufardeci,E., Fabbri,S. and Tocchini-Valentini, G.P. (1992) Participation of the intron in the reaction catalyzed by the *Xenopus* tRNA splicing endonuclease. *Science*, **255**, 1404–1408.

Dahm,S.C., Derrick,W.B. and Uhlenbeck,O.C. (1993) Evidence for the role of the solvated metal hydroxide in the hammerhead cleavage mechanism. *Biochemistry*, **32**, 13040–13045.

Fedor,M.J. and Uhlenbeck,O.C. (1992) Kinetics of intermolecular cleavage by hammerhead ribozymes. *Biochemistry*, **31**, 12042–12054.

Fersht,A. (1985) *Enzyme Structure and Mechanism*. W.H.Freeman and Company, New York, pp. 426–431

Kiersek,R. (1992) Nonenzymatic hydrolysis of oligonucleotides. *Nucleic Acids Res.*, **20**, 5078–5084.

Pan,T., Long,D.M. and Uhlenbeck,O.C. (1993) Divalent metal ions in RNA folding and catalysis. In Gesteland,R.F. and Atkins,J.F. (eds), *The RNA World*. Cold Spring Harbor Laboratory Press, Cold Spring Harbor, NY, pp. 271–302

Pan,T., Dichtl,B. and Uhlenbeck,O.C. (1994) Properties of an *in vitro* selected Pb^{2+} cleavage motif. *Biochemistry*, **33**, 9561–9565.

Phizicky,E.M. and Greer,C.L. (1993) Pre-tRNA splicing: variation on a theme or exception to the rule? *Trends Biochem. Sci.*, **18**, 31–34.

Ruffner,D.E., Stormo,G.D. and Uhlenbeck,O.C. (1990) Sequence requirements of the hammerhead RNA self-cleavage reaction. *Biochemistry*, **29**, 10695–10702.

Weiner,A. and Maizels,N. (1994) Phylogeny from function: evidence from the fossil record that rRNA originated in replication, not translation. *Proc. Natl Acad. Sci. USA*, **91**, 6729–6734.

Received on May 23, 1995; revised on June 26, 1995